RAPID REPORT

Action potential initiation and propagation in hippocampal mossy fibre axons

Christoph Schmidt-Hieber, Peter Jonas and Josef Bischofberger

Physiological Institute 1, University of Freiburg, Hermann-Herder-Strasse 7, D-79104 Freiburg, Germany

Dentate gyrus granule cells transmit action potentials (APs) along their unmyelinated mossy fibre axons to the CA3 region. Although the initiation and propagation of APs are fundamental steps during neural computation, little is known about the site of AP initiation and the speed of propagation in mossy fibre axons. To address these questions, we performed simultaneous somatic and axonal whole-cell recordings from granule cells in acute hippocampal slices of adult mice at ∼23°C. Injection of short current pulses or synaptic stimulation evoked axonal and somatic APs with similar amplitudes. By contrast, the time course was significantly different, as axonal APs had a higher maximal rate of rise (464 ± 30 V s^{-1} in the axon *versus* 297 ± 12 V s^{-1} in the soma, mean ± S.E.M.). Furthermore, analysis of latencies between the axonal and somatic signals showed that APs were initiated in the proximal axon at ∼20–30 μm distance from the soma, and propagated orthodromically with a velocity of 0.24 m s^{-1}. Qualitatively similar results were obtained at a recording temperature of ∼34°C. Modelling of AP propagation in detailed cable models of granule cells suggested that a ∼4 times higher Na^+ channel density (∼1000 pS μm^{-2}) in the axon might account for both the higher rate of rise of axonal APs and the robust AP initiation in the proximal mossy fibre axon. This may be of critical importance to separate dendritic integration of thousands of synaptic inputs from the generation and transmission of a common AP output.

(Received 18 December 2007; accepted after revision 5 February 2008; first published online 7 February 2008)
Corresponding author J. Bischofberger: Physiologisches Institut, Universität Freiburg, Hermann-Herder-Str. 7, D-79104 Freiburg, Germany. Email: josef.bischofberger@uni-freiburg.de

Mammalian central neurons use action-potential (AP)-triggered neurotransmitter release to communicate with each other. Although APs have long been thought of as binary all-or-none signals, more recent evidence suggests that the axonal AP shape and neurotransmitter release are strongly affected by a variety of factors, such as AP frequency and subthreshold membrane potential changes (Geiger & Jonas, 2000; Debanne, 2004; Alle & Geiger, 2006; Shu *et al.* 2006; Kole *et al.* 2007). Moreover, APs are not only output signals, but also propagate back into the dendrites to provide a feedback signal to the input synapses of a given neuron (Stuart *et al.* 1997*a*). To understand how graded synaptic activity is converted into an output signal, it is therefore essential to know where and how APs are initiated within a cell.

Direct axonal measurements of AP initiation and propagation have shown that the proximal axon is the default initiation site in several types of central mammalian neurons, such as neocortical layer V pyramidal cells (Stuart *et al.* 1997*b*; Palmer & Stuart, 2006; Kole *et al.* 2007), cerebellar Purkinje cells (Stuart & Häusser, 1994; Clark *et al.* 2005; Khaliq & Raman, 2006) and CA3 pyramidal neurons (Meeks & Mennerick, 2007). However, dendritic AP initiation has been observed, at least under some conditions, in hippocampal oriens-alveus interneurons (Martina *et al.* 2000), spinal cord motoneurons (Larkum *et al.* 1996) and mitral cells of the olfactory bulb (Chen *et al.* 1997). Moreover, regenerative dendritic potentials have been found in layer V pyramidal cells, but the low density of active conductances and the geometry of these neurons prevents these potentials from fully propagating to the soma and the axon (Stuart *et al.* 1997*b*).

In contrast to the large amount of data that has been obtained in various types of neurons, nothing is known about AP initiation in hippocampal granule cells, mainly because they have particularly thin dendrites and axons inaccessible to direct whole-cell recordings. To overcome these limitations, we performed simultaneous somatic and axonal whole-cell recordings making use of artificial

This paper has online supplemental material.

 DOI: 10.1113/jphysiol.2007.150151

axonal endings that arose from the slicing procedure (Shu *et al.* 2006) and examined action potential initiation and propagation in hippocampal mossy fibre axons.

Methods

Slice preparation

Transverse 350 μm-thick slices were cut from the hippocampus of 2- to 4-month-old C57BL/6 mice using a custom-made vibratome (Geiger *et al.* 2002). Animals were kept in an oxygenated chamber for 10 min, anaesthetized with isoflurane (Forene, Abbott, Germany; 4–5% added to the inspiration air flow) and subsequently killed by decapitation, in accordance with national and institutional guidelines. Experiments were approved by the Animal Care Committee of Freiburg (registry T-05/25). For the dissection and the storage of the slices, a solution containing 87 mM NaCl, 25 mM $NaHCO_3$, 2.5 mM KCl, 1.25 mM NaH_2PO_4, 25 mM glucose, 75 mM sucrose, 7 mM $MgCl_2$ and 0.5 mM $CaCl_2$ (equilibrated with 95% O_2–5% CO_2) was used. Slices were incubated at 35°C for 30 min and subsequently stored at room temperature.

Electrophysiology

Slices were superfused with a physiological extracellular solution containing 125 mM NaCl, 25 mM $NaHCO_3$, 2.5 mM KCl, 1.25 mM NaH_2PO_4, 25 mM glucose, 2 mM $CaCl_2$, 1 mM $MgCl_2$ and 10 μM bicuculline methiodide (equilibrated with 95% O_2–5% CO_2). Spontaneous synaptic excitation was blocked with 10 μM 6-cyano-7-nitroquinoxaline-2,3-dione (CNQX) except in experiments with evoked excitatory synaptic potentials. Mature granule cells and terminal axonal expansions resulting from the slicing procedure (bleb diameter: ~2–3 μm; Shu *et al.* 2006) were identified using infrared differential interference contrast (IR-DIC) video microscopy. Whole-cell patch-clamp recordings from axonal blebs were established under IR-DIC control using a pipette solution containing 100 μM Alexa594 (Invitrogen, Carlsbad, CA, USA). Subsequently, the fluorescently labelled soma was identified using a CCD camera (EBFT 512; Princeton Instruments, Trenton, NJ, USA). The excitation light source (Polychrome II; T.I.L.L. Photonics, Munich, Germany) was coupled to the epifluorescent port of the microscope (Axioskop FS2: Zeiss, Jena, Germany; ×60 water immersion objective: Olympus, Tokyo, Japan) via a light guide. To minimize bleaching and phototoxicity, the intensity of the excitation light (550 nm) was reduced to 10%. During illumination with this intensity, no obvious change in AP properties of granule cells was observed. Patch pipettes (6–10 MΩ for somatic recordings, 6–15 MΩ for axonal and dendritic recordings) were pulled from thick-walled borosilicate glass (outer diameter, 2.0 mm; inner diameter, 0.6 mm) to minimize pipette capacitance (Bischofberger *et al.* 2006). Voltage signals were measured with a Multiclamp 700A amplifier (Molecular Devices, Palo Alto, CA, USA), filtered at 10 kHz and digitized at 20 kHz using a CED 1401plus interface (Cambridge Electronic Design, Cambridge, UK). Current pulses were generated using home-made data acquisition software (FPulse) running under Igor 5 (WaveMetrics, Lake Oswego, OR, USA). Pipettes were filled with a solution containing 120 mM potassium gluconate, 20 mM KCl, 10 mM EGTA, 2 mM $MgCl_2$, 2 mM Na_2ATP, 0.3 mM NaGTP, 1 mM sodium phosphocreatine and 10 mM Hepes (pH adjusted to 7.2 with KOH). Pipette capacitance and series resistance of 20–40 MΩ (somatic recordings) or 25–65 MΩ (axonal recordings) were compensated. To stimulate the perforant path fibres, pipettes were filled with 1 M NaCl solution and placed in the outer molecular layer. Low-intensity stimulation (200 μs pulses; ~5 V) was adjusted so that excitatory postsynaptic potentials (EPSPs) were slightly above AP threshold. For high-intensity stimulation (200 μs pulses; ~25 V), stimulus amplitude was increased until no further decrease in the latency between the stimulation artefact and the first AP could be detected. Holding potential was −80 mV. Recordings were performed at 22–24°C except when stated differently.

Data analysis

Fluorescent labelling and morphological reconstructions of granule cells were performed as previously described (Schmidt-Hieber *et al.* 2007). For details see online Supplemental material. AP amplitudes were measured from the holding potential of −80 mV. AP latencies were measured as the difference in time at half-maximal amplitudes. Negative values denote APs preceding the somatic AP. The AP latencies (L) shown in Fig. 3*A* and *B* were fitted with the function:

$$L(x) = [1 - f(x)]m_1x + f(x)(m_2x + c), \quad (1)$$

where x is the distance from the soma, m_1 and m_2 are slopes of linear functions and c is a y-intercept. $f(x)$ is a Boltzmann function of the form:

$$f(x) = 1/\{1 + \exp[(h - x)/k]\}, \quad (2)$$

where h and k are the midpoint and slope, respectively. The two linear functions are each multiplied with Boltzmann functions to describe the transition between somatodendritic and axonal propagation. The axonal propagation velocity v was determined as $v = 1/m_2$. Compartmental modelling was performed with NEURON 6.0 (Carnevale & Hines, 2006) as previously described (Engel & Jonas, 2005; Schmidt-Hieber *et al.* 2007). For details see Supplemental material. A non-parametric Wilcoxon signed-rank test was used to assess statistical significance. Values are given as mean ± S.E.M.

Error bars in the figures also indicate the s.e.m. Data were analysed using C-Stimfit (C. S.-H), Gnumeric and GNU R.

Results

APs evoked by current injections are initiated in granule cell axons

To determine the site of AP initiation, we performed simultaneous whole-cell patch-clamp recordings from the soma and the axon of mature hippocampal granule cells in brain slices from 2- to 4-month-old mice (Fig. 1; Schmidt-Hieber *et al.* 2004). As granule cells have particularly thin axons with a diameter of less than 0.3 μm (Geiger *et al.* 2002), we recorded from artificial terminal axonal expansions ('blebs') that arose from the slicing procedure at distances of 6–97 μm from the border of the soma in the presence of the synaptic blockers bicuculline and CNQX (10 μM each; Fig. 1*A*; Shu *et al.* 2006).

When short current pulses (0.5 ms; 1.5–3.0 nA) were applied at the soma of granule cells, axonal APs preceded somatic APs in 23 of 26 recordings (Fig. 1*B* and *C*). Axonal and somatic APs had similar amplitudes (132 ± 2 *versus* 135 ± 1 mV, mean $\pm$ s.e.m.; Fig. 1*F*) and half-durations (2.1 ± 0.0 *versus* 1.8 ± 0.0 ms; $n = 22$; Fig. 1*G*). However, axonal APs preceded somatic APs with a mean latency of -144 ± 22 μs ($n = 26$; Fig. 1*H*). Omitting bicuculline from the bath solution did not significantly affect the negative AP latencies between axon and soma (103.9 ± 5.0% of control; $P > 0.5$; $n = 3$), indicating that the low levels of spontaneous synaptic inhibition did not change AP initiation and propagation. When the injection

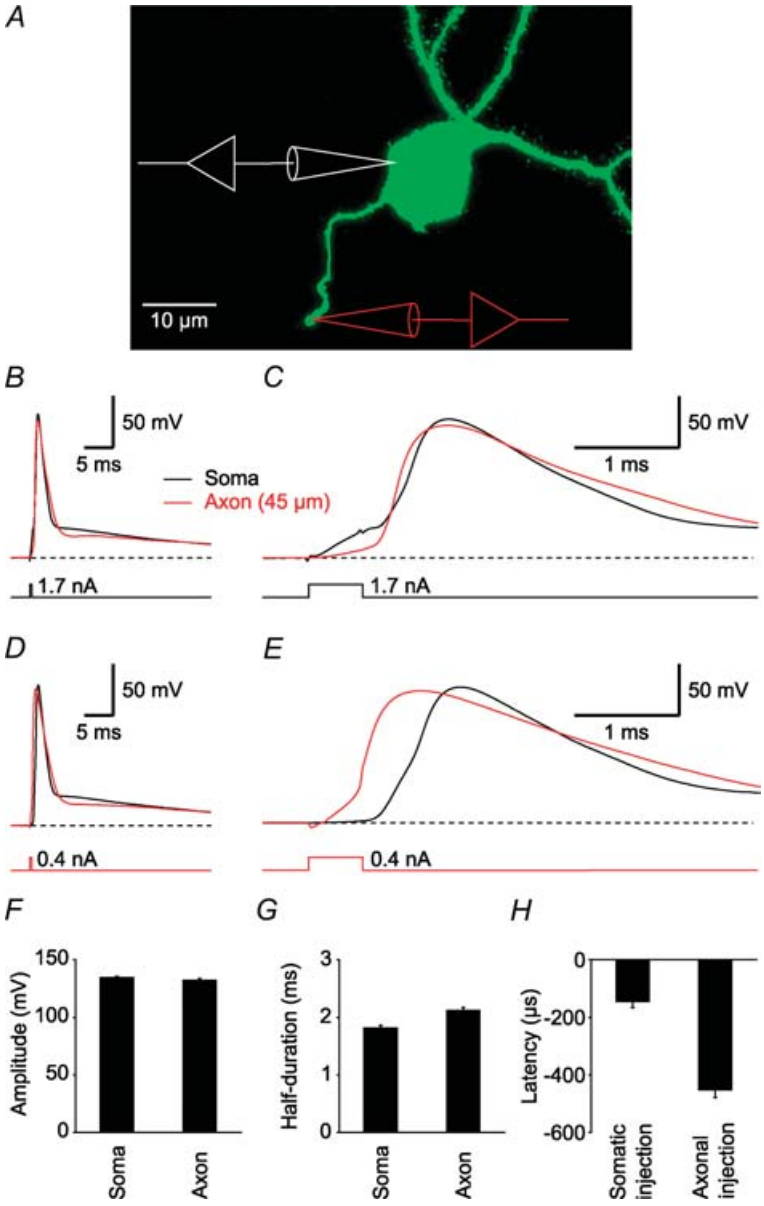

Figure 1. Robust axonal AP initiation is independent of the site of current injection
A, projection of a stack of fluorescence images taken from a hippocampal granule cell. The cell was filled with biocytin during whole-cell recording and subsequently labelled with FITC–avidin. *B*, the traces show an AP evoked by brief current injections to the soma, recorded simultaneously in an axonal bleb (red trace) and in the soma (black trace). *C*, the same AP as in *B* was plotted at an expanded time scale. *D* and *E*, same cell as in *B*, but the current was injected into the axon. *F* and *G*, summary bar graphs comparing the AP amplitudes (*F*) and half-durations (*G*) in the soma and axon. *H*, summary bar graph showing the AP latencies between axon and soma.

site was swapped to the axon (0.5 ms; 0.3–1.0 nA; Fig. 1*D* and *E*), axonal APs preceded somatic APs with a latency of -452 ± 27 μs ($n = 23$; Fig. 1*H*). These results indicate that APs are robustly initiated in granule cell axons, independently of the site of current injection.

Axonal AP initiation upon synaptic stimulation

To analyse AP initiation during synaptic excitation, we used extracellular synaptic stimulation of the perforant path and recorded voltage responses simultaneously in the soma and the axon of a granule cell (Fig. 2). In 5 out of 5 cells, axonal APs preceded somatic APs (Fig. 2*A*). When either short somatic current pulses or extracellular synaptic stimulation were used to evoke APs in the same cells, no significant difference in AP latencies could be found (-191 ± 40 μs *versus* -188 ± 10 μs; $n = 5$; $P > 0.5$; Fig. 2*B*). To test whether increasing synaptic stimulation intensity affected AP initiation, we compared APs evoked by low- and high-intensity synaptic stimulation in the same cells. Again, APs in the axon preceded somatic APs ($n = 4$), regardless of synaptic stimulation strength (Fig. 2*C*). With high-intensity stimulation, a consistent decrease in latencies was observed (-211 ± 25 μs *versus* -142 ± 26 μs; $n = 4$; $P < 0.05$, one-tailed Wilcoxon signed-rank test; Fig. 2*D*). This indicates that during maximal synaptic stimulation, the strong subthreshold depolarization reduces the time until a somatic AP reaches 50% of its maximal amplitude. Nevertheless, latencies always remained negative, indicating axonal initiation. Finally, when the recording temperature was increased to ~34°C, the APs were also initiated in the axon with a latency of -107 ± 25 μs ($n = 3$) using brief somatic current injections and -136 ± 25 μs or -122 ± 26 μs ($n = 3$) using low- or high-intensity synaptic stimulation. Taken together, the data show that suprathreshold excitatory synaptic activity in granule cells consistently leads to axonal AP initiation rather than local dendritic spike initiation.

APs are initiated close to the granule cell soma

In various types of central neurons, APs have been shown to be initiated at different axonal locations between the axon hillock and the first node of Ranvier. Furthermore, axonal propagation velocity in different cell types varies within a wide range. To determine the exact site of initiation and the propagation velocity of APs in mossy fibre axons, we analysed latencies measured at various distances from the soma when short current pulses were injected into the soma (Fig. 3*A*). The greatest negative time differences between somatic and axonal APs occurred at a distance of ~20–30 μm from the soma, indicating that this latency minimum was the site of AP initiation (Fig. 3*B*). The latencies could be fitted with a function describing the different propagation velocities in the axonal and somatodendritic domain (see Methods, eqn (1)). According to the best-fit parameters, the orthodromic propagation velocity in the axon was 0.24 m s^{-1}. We performed the same analysis using axonally evoked APs (Fig. 3*C*). In this case, the data showed no apparent latency minimum, suggesting that APs were initiated close to the axonal site of current injection and propagated antidromically with a velocity of about

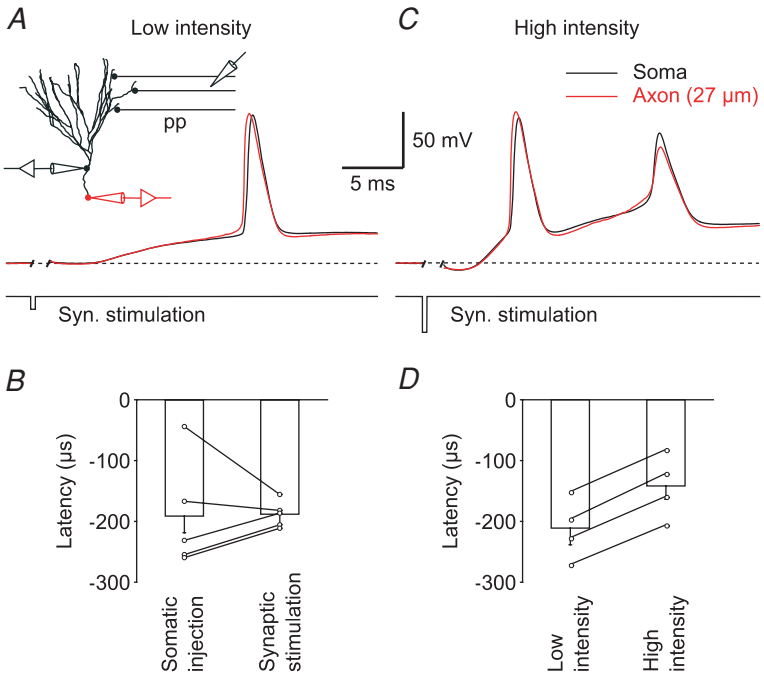

Figure 2. Robust axonal AP initiation following synaptic stimulation
A, the traces show an AP evoked by low-intensity extracellular synaptic stimulation of the lateral perforant path (pp). *B*, bar graph showing AP latencies between axon and soma when currents were injected into the soma or after extracellular synaptic stimulation of the perforant path ($n = 5$; $P > 0.5$). *C*, the traces show an AP evoked by high-intensity extracellular synaptic stimulation. *D*, bar graph showing AP latencies between axon and soma with low- or high-intensity synaptic stimulation ($n = 4$).

$-0.21\ \mathrm{m\,s^{-1}}$, similar to what was observed in the other direction (Fig. 3*D*). These data indicate that granule cell axons are highly excitable and that the default initiation site is located in the proximal axon, close to the granule cell soma.

The maximal slope of rise of APs is steeper in the axon than in the soma

The maximal slope of rise ($\mathrm{d}V/\mathrm{d}t_{max}$) of APs depends on the available Na^+ conductance. Since Na^+ channel densities in the axon and the soma of various types of neurons have been suggested to differ by several orders of magnitude (Mainen *et al.* 1995), we compared $\mathrm{d}V/\mathrm{d}t_{max}$ in the soma and the axon of granule cells (Fig. 3*E*). On average, axonal APs had a significantly higher rate of rise ($464 \pm 30\ \mathrm{V\,s^{-1}}$) than somatic APs ($297 \pm 12\ \mathrm{V\,s^{-1}}$; $n = 22$; $P < 0.01$; Fig. 3*F*) consistent with a higher density of Na^+ channels. The contribution of voltage-gated K^+ channels to the rate of rise is likely to be small, as it was shown in mossy fibre boutons and in pyramidal cell axons that these channels affect the AP repolarization rather than the depolarization phase (Geiger & Jonas, 2000; Kole *et al.* 2007). Furthermore, when we varied the holding potential from −90 mV to −60 mV using hyperpolarizing or depolarizing current pulses, the maximal rate of rise in the axon did not increase with depolarization (via inactivation of A-type K^+ channels), but rather decreased to $77.3 \pm 9.6\%$ at −60 mV ($n = 3$). Taken together, K^+ channels probably do not play a major role in shaping the upstroke of APs in dentate gyrus granule cells, suggesting that the difference in AP rise time is due to a higher Na^+ channel density in the axon than in the soma. Furthermore, these data indicate that a higher density of axonal Na^+ channels might not only shape the time course of axonal APs, but also contribute to axonal AP initiation.

Higher Na^+ conductance density supports robust axonal AP initiation

To obtain a quantitative estimate of peak Na^+ conductance densities ($\bar{g}_{Na}$), we performed a computational analysis of spike initiation in granule cells based on a detailed compartmental cable model (Fig. 4). A previously

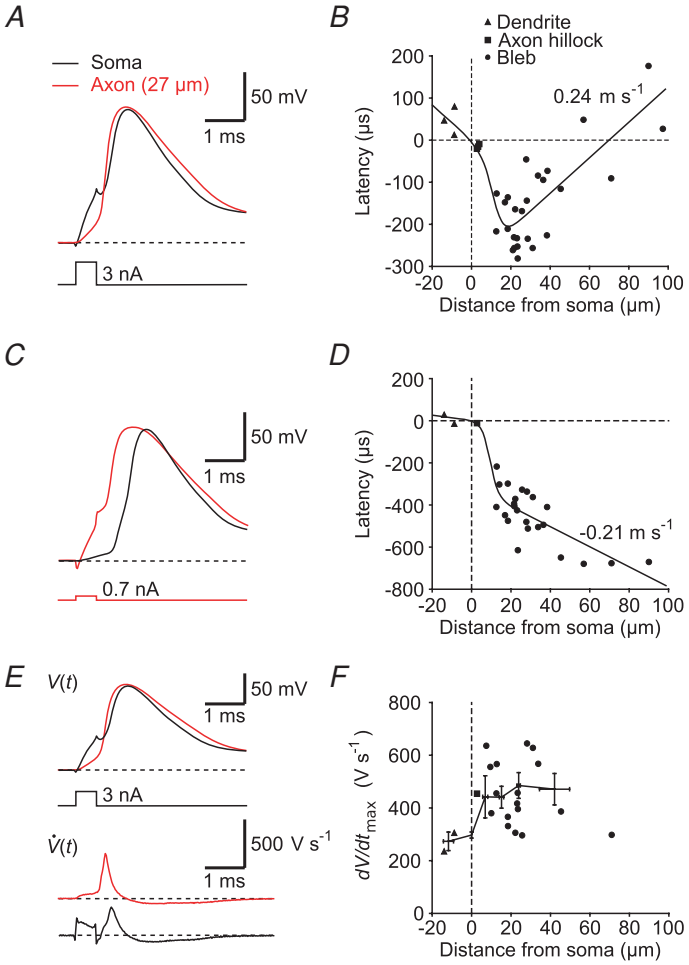

Figure 3. The AP initiation site is located in the proximal mossy fibre axon
A, AP recorded at the soma (black trace) and in the axon (red trace) evoked by a brief somatic current injection. *B*, plot of AP latencies against distance from soma, measured in proximal dendritic shafts, axon hillocks or axonal blebs after brief somatic current injection. The continuous curve represents a function fitted to the data (see Methods, eqn (1)). The most negative latencies were measured at ~20 μm distance from the soma. *C* and *D*, same as in *A* and *B*, but current was injected into the axon. *E*, the upper traces ($V(t)$) show the same AP as in *A*. The lower traces show the differentiated voltage signal ($\dot{V}(t)$). *F*, plot of the maximal rate of rise ($\mathrm{d}V/\mathrm{d}t_{max}$) of APs against distance from soma. The black circles represent binned averages with error bars. Axonal APs had a significantly higher rate of rise than somatic APs ($n = 22$; $P < 0.01$).

developed passive cable model (Schmidt-Hieber *et al.* 2007; Fig. 4*A*) was used as a skeleton into which kinetic models of Na^+ and K^+ conductances were inserted (Engel & Jonas, 2005). The maximal conductance densities $\bar{g}_{Na}$ and $\bar{g}_K$ were fitted to minimize the sum of squared errors between dV/dt_{max} during the rise and decay of simulated and experimentally measured APs. When $\bar{g}_{Na}$ was assumed to be uniformly distributed throughout soma, dendrites and axon (36 mS cm^{-2}), we could fit neither the axonal nor the somatic maximal slope of rise (Fig. 4*B*, grey bars). However, using independent $\bar{g}_{Na}$ for the somatodendritic (27 mS cm^{-2}) and the axonal domain (96 mS cm^{-2}) resulted in a ~75-fold smaller sum of squared errors, and we could precisely reproduce the maximal slopes of rise at different subcellular compartments (Fig. 4*B*, black bars; Fig. 4*C*). In good agreement with the experimental data, the non-uniform model predicted an AP initiation site at 28 μm distance from the soma and an orthodromic propagation velocity of 0.23 m s^{-1} (Fig. 4*D*). The apparent AP initiation site was independent of whether a cut axon with a terminal bleb or an intact axon of 1 mm length was used in the model. The robust axonal initiation of APs is further demonstrated by a more detailed analysis of the initial phase of the AP (Fig. S1, Supplemental material) showing that depolarization of the axon precedes the soma for all points of the rising phase above a threshold of about $V_m = -55$ mV.

To test whether the higher Na^+ conductance density in the axon would contribute to the robust axonal AP initiation upon synaptic stimulation, we simulated excitatory synaptic conductance changes to evoke APs (Fig. 4*E*). A total number of six synapses distributed along a single dendrite evoked APs with peak synaptic conductances larger than ~0.4 nS each. Similar to our experimental data (Fig. 2), APs were always initiated in the axon when $\bar{g}_{Na}$ was non-uniformly distributed according

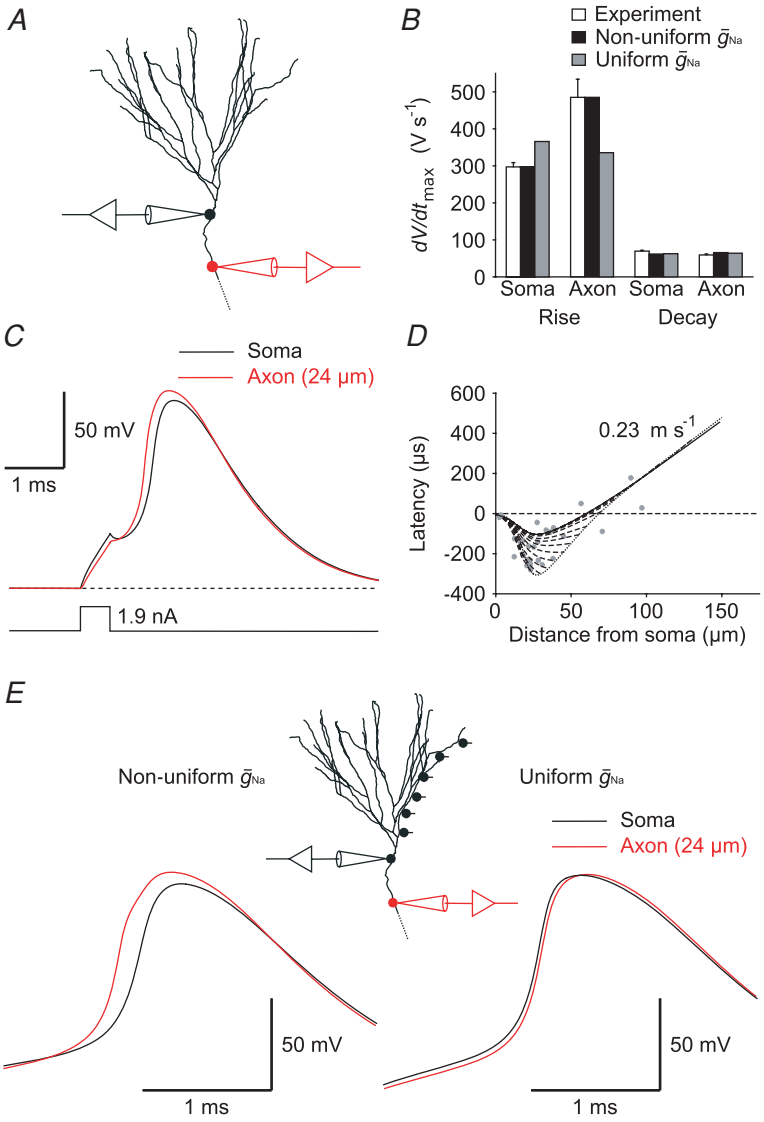

Figure 4. Simulation of AP initiation and propagation in a detailed compartmental model of a granule cell
A, shape plot of a granule cell (cell 7 from Schmidt-Hieber *et al.* 2007) generated with NEURON. *B*, the bar graph shows the maximal rate of rise and the maximal rate of decay of APs. Experimental data (white bars) were taken from recordings at a distance of 20–30 μm from soma (mean distance from soma: 24 ± 1 μm; max. slope during rise: 297 ± 12 V s^{-1} (soma), 485 ± 49 V s^{-1} (axon); max. slope during decay: 70 ± 2 V s^{-1} (soma), 59 ± 2 V s^{-1} (axon)). Models were obtained using either non-uniform peak Na^+ conductance densities ($\bar{g}_{Na}$) in the somatodendritic and axonal domains (black bars) or a uniformly distributed $\bar{g}_{Na}$ (grey bars). *C*, traces show a simulated AP recorded at the soma (black trace) and in the axon (red trace) at 24 μm distance from the soma. *D*, simulated AP latencies were plotted against distance from soma. The most negative latencies were observed at ~28 μm distance from soma. In addition to an intact axon (continuous curve), results from simulations using axons with variable lengths and a bleb (diameter: 2.5 μm; length: 3 μm) at the end are shown as dashed curves. The dotted curve connects the end points of these lines. Grey points represent measured data. *E*, traces show simulated APs evoked by excitatory synaptic conductance changes (6 synapses distributed along a dendritic path; see inset). $\bar{g}_{Na}$ was either non-uniformly (left traces) or uniformly (right traces) distributed in the somatodendritic and axonal domains.

to our best-fit parameters (Fig. 4*E*). This behaviour could not be replicated when $\bar{g}_{Na}$ was uniform throughout the cell. Together, these simulations suggest that the Na^+ channel conductance density is ∼4 times higher in the axon than in the soma, leading to a robust axonal initiation site.

Discussion

Our results determine, for the first time, the AP initiation site and propagation velocity in hippocampal granule cells. We found that APs are initiated in the axon upon both current injections and suprathreshold synaptic stimulation. The initiation site is located at ∼20–30 μm distance from the soma and APs propagate orthodromically with a velocity of ∼0.24 m s^{-1}. Finally, detailed computional analysis of AP initiation and propagation suggested that a ∼4 times higher Na^+ channel density in the axon can fully account for the robust axonal initiation.

APs are initiated close to the axon hillock

Several recent studies using simultaneous recordings from the axon and the soma of central mammalian neurons have provided evidence that the AP initiation site is located in the proximal axon, similar to our findings. However, the exact location within the proximal axon seems to depend on the type of neuron, ranging from the axon initial segment in neocortical layer V and hippocampal CA3 pyramidal cells (∼30–40 μm distance from the soma; Palmer & Stuart, 2006; Kole *et al.* 2007; Meeks & Mennerick, 2007) to the first node of Ranvier in cerebellar Purkinje cells (∼75 μm distance from the soma; Clark *et al.* 2005). This diversity may be explained by differences in somatodendritic and axonal Na^+ channel densities, cell geometry and myelination. In the unmyelinated mossy fibre axon, we find that the initiation site is located at ∼20–30 μm distance from the soma. A possible explanation for this very proximal location might be that the particularly small diameter of these axons (< 0.3 μm, Geiger *et al.* 2002) increases the electrotonic distance between the soma and proximal axonal compartments, thereby isolating the initiation site from the large capacitance of the soma. A high Na^+ conductance density at the initiation site would then charge the axonal membrane more effectively because of the substantially smaller electrical load as compared to that for a thicker axon (Mainen *et al.* 1995; Palmer & Stuart, 2006).

High Na^+ channel density at the initiation site in mossy fibre axons

Our results indicate that Na^+ channel density is high in the initial part of the axon. While simulation and labelling studies suggest that there is a 7- to 1000-fold higher density of Na^+ channels at the axonal initiation site (Wollner & Catterall, 1986; Mainen *et al.* 1995), direct patch-clamp recordings from somatic and axonal membranes have initially not confirmed this finding (Colbert & Johnston, 1996; Colbert & Pan, 2002). However, recently it has been shown in neocortical pyramidal cells that Na^+ currents were substantially larger in axonal membrane patches as compared to patches from somata (Kole *et al.* 2008). Using a detailed compartmental model of a hippocampal granule cell, we could accurately reproduce the rates of rise of the AP, the proximal initiation site and the propagation velocity with a peak Na^+ conductance density ($\bar{g}_{Na}$) that was ∼4 times higher in the axon than in the soma. By contrast, we failed to replicate our experimental findings assuming a uniform distribution of $\bar{g}_{Na}$ throughout the cell.

According to our model, we would expect $\bar{g}_{Na}$ to be ∼100 mS cm^{-2} (corresponding to 1000 pS μm^{-2}) in the axon, which is comparable to that in non-myelinated invertebrate axons (120 mS cm^{-2} in squid axons; Hodgkin & Huxley, 1952), but substantially larger than in mossy fibre boutons, the large presynaptic terminals of granule cell axons (49 mS cm^{-2}; Engel & Jonas, 2005). However, as our analysis was restricted to the proximal 100 μm of the axon, the data would also be consistent with a 'hot spot' of Na^+ channels clustered around the initiation site and smaller Na^+ channel densities at more distal parts of the axon.

A stable initiation site may be important for temporal coding

Previously, we have shown that granule cells have a compact electrotonic structure that enables efficient somatodendritic propagation of passive voltage signals for frequencies of up to ∼75 Hz (Schmidt-Hieber *et al.* 2007). Therefore, one might expect that the granule cell dendritic tree constitutes a single computational unit for the integration of synaptic potentials. On the other hand, the presence of active conductances might substantially alter signal integration or even result in local AP initiation within individual dendritic branches. However, none of the protocols used to evoke APs was capable to shift the initiation site away from the proximal axon, demonstrating that the mechanisms generating APs are robust and stable. Therefore, excitatory and inhibitory synaptic inputs in individual dendrites are integrated, and if the AP threshold is reached, a common output is generated in the initial axon close to the soma.

Our results have several functional implications for the conversion of synaptic input into axonal output in hippocampal granule cells. First, all excitatory synaptic connections with similar peak conductance, but different dendritic locations, will equivalently contribute to

AP output, because their subthreshold somatic EPSP amplitude is similar (Schmidt-Hieber *et al.* 2007). Second, if the AP had been generated at variable sites within the dendritic tree, its timing and shape would have been expected to be variable as well. By contrast, the stable initiation site supports a stereotypic AP shape and time course of AP propagation. Finally, a stable, proximal axonal initiation site places perisomatic inhibition in a powerful position for modulating AP output (McBain & Fisahn, 2001; Bartos *et al.* 2007). In particular, basket cells and axo-axonic cells effectively inhibit glutamatergic principal cells during hippocampal theta–gamma oscillations (Somogyi & Klausberger, 2005). Oscillating networks of basket cells might therefore be able to entrain the timing of AP output in large granule cell populations with high temporal precision and large efficacy (Bartos *et al.* 2007). Thus, the stable initiation in the proximal axon provides a binary output signal which carries information mainly by timing and rate of largely uniform APs.

References

Alle H & Geiger JRP (2006). Combined analog and action potential coding in hippocampal mossy fibers. *Science* **311**, 1290–1293.

Bartos M, Vida I & Jonas P (2007). Synaptic mechanisms of synchronized gamma oscillations in inhibitory interneuron networks. *Nat Rev Neurosci* **8**, 45–56.

Bischofberger J, Engel D, Li L, Geiger JRP & Jonas P (2006). Patch-clamp recording from mossy fiber terminals in hippocampal slices. *Nat Protoc* **1**, 2075–2081.

Carnevale T & Hines M (2006). *The NEURON Book*. Cambridge University Press, Cambridge, UK.

Chen WR, Midtgaard J & Shepherd GM (1997). Forward and backward propagation of dendritic impulses and their synaptic control in mitral cells. *Science* **278**, 463–467.

Clark BA, Monsivais P, Branco T, London M & Häusser M (2005). The site of action potential initiation in cerebellar Purkinje neurons. *Nat Neurosci* **8**, 137–139.

Colbert CM & Johnston D (1996). Axonal action-potential initiation and Na^+ channel densities in the soma and axon initial segment of subicular pyramidal neurons. *J Neurosci* **16**, 6676–6686.

Colbert CM & Pan E (2002). Ion channel properties underlying axonal action potential initiation in pyramidal neurons. *Nat Neurosci* **5**, 533–538.

Debanne D (2004). Information processing in the axon. *Nat Rev Neurosci* **5**, 304–316.

Engel D & Jonas P (2005). Presynaptic action potential amplification by voltage-gated Na^+ channels in hippocampal mossy fiber boutons. *Neuron* **45**, 405–417.

Geiger JRP, Bischofberger J, Vida I, Fröbe U, Pfitzinger S, Weber HJ, Haverkampf K & Jonas P (2002). Patch-clamp recording in brain slices with improved slicer technology. *Pflugers Arch* **443**, 491–501.

Geiger JRP & Jonas P (2000). Dynamic control of presynaptic Ca^{2+} inflow by fast-inactivating K^+ channels in hippocampal mossy fiber boutons. *Neuron* **28**, 927–939.

Hodgkin AL & Huxley AF (1952). A quantitative description of membrane current and its application to conduction and excitation in nerve. *J Physiol* **117**, 500–544.

Khaliq ZM & Raman IM (2006). Relative contributions of axonal and somatic Na channels to action potential initiation in cerebellar Purkinje neurons. *J Neurosci* **26**, 1935–1944.

Kole MHP, Ilschner SU, Kampa BM, Williams SR, Ruben PC & Stuart GJ (2008). Action potential generation requires a high sodium channel density in the axon initial segment. *Nat Neurosci* **11**, 178–186.

Kole MHP, Letzkus JJ & Stuart GJ (2007). Axon initial segment Kv1 channels control axonal action potential waveform and synaptic efficacy. *Neuron* **55**, 633–647.

Larkum ME, Rioult MG & Lüscher HR (1996). Propagation of action potentials in the dendrites of neurons from rat spinal cord slice cultures. *J Neurophysiol* **75**, 154–170.

McBain CJ & Fisahn A (2001). Interneurons unbound. *Nat Rev Neurosci* **2**, 11–23.

Mainen ZF, Joerges J, Huguenard JR & Sejnowski TJ (1995). A model of spike initiation in neocortical pyramidal neurons. *Neuron* **15**, 1427–1439.

Martina M, Vida I & Jonas P (2000). Distal initiation and active propagation of action potentials in interneuron dendrites. *Science* **287**, 295–300.

Meeks JP & Mennerick S (2007). Action potential initiation and propagation in CA3 pyramidal axons. *J Neurophysiol* **97**, 3460–3472.

Palmer LM & Stuart GJ (2006). Site of action potential initiation in layer V pyramidal neurons. *J Neurosci* **26**, 1854–1863.

Schmidt-Hieber C, Jonas P & Bischofberger J (2004). Enhanced synaptic plasticity in newly generated granule cells of the adult hippocampus. *Nature* **429**, 184–187.

Schmidt-Hieber C, Jonas P & Bischofberger J (2007). Subthreshold dendritic signal processing and coincidence detection in dentate gyrus granule cells. *J Neurosci* **27**, 8430–8441.

Shu Y, Hasenstaub A, Duque A, Yu Y & McCormick DA (2006). Modulation of intracortical synaptic potentials by presynaptic somatic membrane potential. *Nature* **441**, 761–765.

Somogyi P & Klausberger T (2005). Defined types of cortical interneurone structure space and spike timing in the hippocampus. *J Physiol* **562**, 9–26.

Stuart G & Häusser M (1994). Initiation and spread of sodium action potentials in cerebellar Purkinje cells. *Neuron* **13**, 703–712.

Stuart G, Schiller J & Sakmann B (1997*b*). Action potential initiation and propagation in rat neocortical pyramidal neurons. *J Physiol* **505**, 617–632.

Stuart G, Spruston N, Sakmann B & Häusser M (1997*a*). Action potential initiation and backpropagation in neurons of the mammalian CNS. *Trends Neurosci* **20**, 125–131.

Wollner DA & Catterall WA (1986). Localization of sodium channels in axon hillocks and initial segments of retinal ganglion cells. *Proc Natl Acad Sci U S A* **83**, 8424–8428.

Acknowledgements

We thank Jörg Geiger for helpful discussions and carefully reading the manuscript. We also thank S. Becherer, M. Northemann and K. Winterhalter for technical assistance. This work was supported by grants from the Deutsche Forschungsgemeinschaft (Bi 642/2, SFB 505 and SFB 780).

Supplemental material

Online supplemental material for this paper can be accessed at:
http://jp.physoc.org/cgi/content/full/jphysiol.2007.150151/DC1
and
http://www.blackwell-synergy.com/doi/suppl/10.1113/jphysiol.2007.150151